



37

38 **Keywords:** ultraviolet germicidal irradiation; SARS-CoV-2; indoor air quality; photochemistry;  
39 ventilation; airborne disease transmission

40

41 **Synopsis:** Germicidal ultraviolet light initiates indoor oxidation chemistry, potentially forming  
42 indoor air pollutants. The amount is not negligible and depends on both the wavelength of light  
43 and the ventilation level.

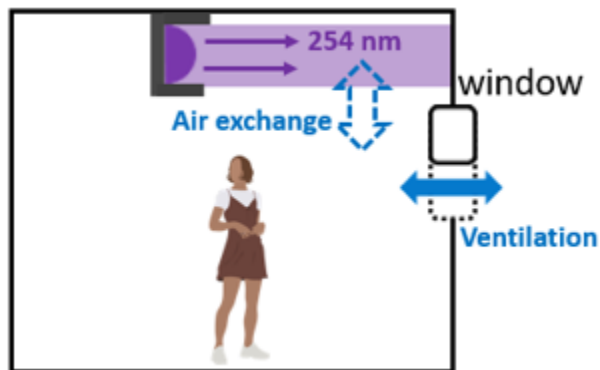
44

## 45 Introduction

46 Germicidal ultraviolet light (GUV) has been employed to disinfect air in indoor spaces since the  
47 1930s.<sup>1</sup> It has been shown to effectively limit the airborne transmission of infectious diseases,  
48 e.g., measles and tuberculosis.<sup>1-3</sup> This is due to photon-induced dimerization of pyrimidines in  
49 the nucleic acids of airborne pathogens (and loss of their ability to replicate as a result). GUV  
50 fixtures use lamps that emit in the UVC range, most commonly at 254 nm (hereinafter  
51 “GUV254”).<sup>4</sup> As 254 nm UV can cause skin and eye irritation,<sup>5</sup> GUV254 is usually applied near  
52 the ceiling (Figure 1a) or inside ventilation ducts. Recently, 222 nm UV has been shown to not  
53 only have strong capability of inactivating airborne viruses,<sup>6</sup> but also is claimed to be safe to  
54 humans<sup>7</sup> (although this is controversial),<sup>8</sup> potentially allowing whole-room GUV applications  
55 (“GUV222”) (Fig. 1b). Ground-resting GUV-based air cleaners have also been commercialized,  
56 in which a fan continuously pulls air into a box and exposes it to UV light, from which the  
57 occupants are shielded.<sup>9</sup>

58

59 (a)



60

61

62

63

64

65

66

67

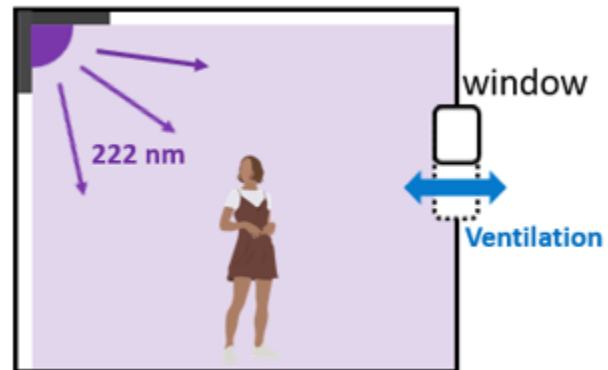
68

69

70

71

(b)



72 (c)

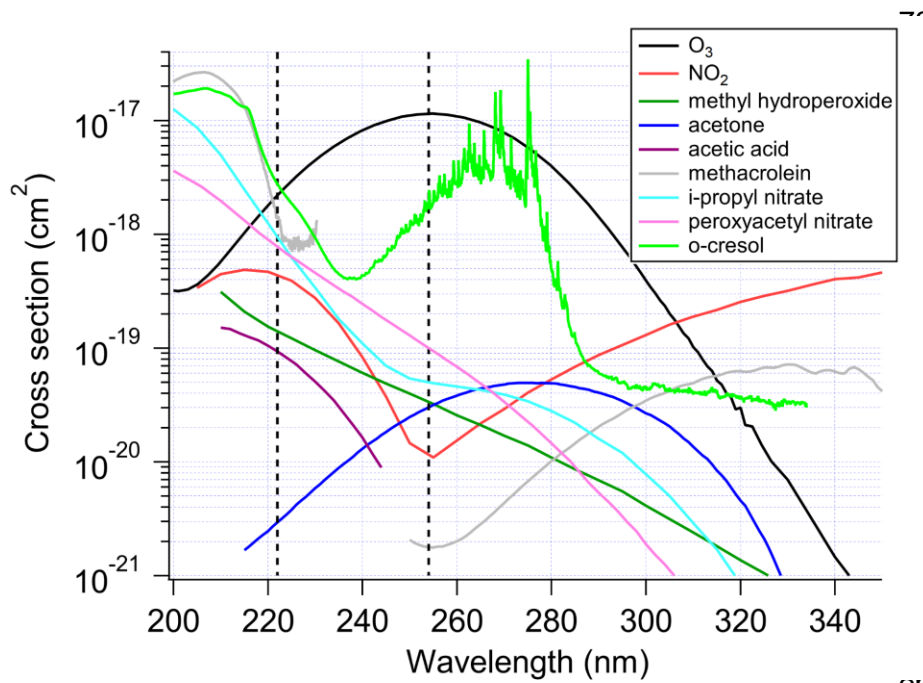


**Figure 1.**

Schematics of a germicidal ultraviolet air disinfection system at (a) 254 nm and at (b) 222 nm in a room; (c) absorption cross sections of several important gas-phase species relevant to this study (a discontinuity in the spectrum of

87 *methacrolein is due to lack of data*).

88

89 During the COVID-19 pandemic, GUV has drawn renewed interest as a tool for airborne virus  
90 inactivation. Inhalation of airborne virus is widely accepted as the main transmission route of  
91 COVID-19,<sup>10-12</sup> which explains the dominant indoor character of transmission.<sup>13</sup> An important  
92 component of the transmission is due to superspreading events,<sup>14</sup> which have been shown to be  
93 mostly explained by shared-room airborne transmission.<sup>15</sup> Much transmission also happens in  
94 close proximity due to short-range airborne transmission, but even in this situation a substantial  
95 fraction of the inhaled virus may come from well-mixed room air.<sup>16,17</sup> As COVID-19 remains  
96 widespread, and with the possible appearance of new variants, there is a pressing need to  
97 remove inhalable viruses from indoor environments.<sup>3</sup> Similar measures would be beneficial for  
98 other airborne diseases such as tuberculosis, measles, or a future pandemic virus.

99

100 Physical measures such as (natural and/or mechanical) ventilation and air filtration have been  
101 proven safe and effective.<sup>18</sup> Nevertheless, mechanical ventilation and air filtration usually can  
102 remove airborne pathogens only at a few effective air changes per hour (ACH)<sup>19</sup> and natural  
103 ventilation can be highly variable and impractical depending on weather, or when pollution,  
104 allergens or noise are present outdoors. When a high virus removal rate (e.g., >10 ACH) needs

105 to be ensured (e.g., in high-risk environments), GUV emerges as a practical and potentially  
106 cost-effective way to achieve it.<sup>3,18</sup>

107  
108 UVC light is known to generate strong oxidants (e.g., OH radicals, and sometimes also O<sub>3</sub>  
109 depending on the wavelengths used),<sup>20</sup> which can subsequently oxidize volatile organic  
110 compounds (VOCs) indoors and initiate organic radical chemistry in indoor air.<sup>21,22</sup> Energetic  
111 UVC photons can also directly photolyze many VOCs, such as peroxides<sup>23,24</sup> and carbonyls,<sup>25,26</sup>  
112 and generate organic radicals. This radical chemistry is thought to lead to further oxidation of  
113 indoor VOCs and the formation of oxygenated VOCs (OVOCs) and secondary organic aerosol  
114 (SOA), both of which may have negative health effects.<sup>27</sup> Surveys of the concentration of total  
115 VOCs in the indoor environments range from ~0.1-4 mg m<sup>-3</sup>.<sup>28-30</sup> Thus there is always a  
116 significant amount of VOC to react with any radicals and oxidants that are generated indoors,  
117 and any “air cleaning” technique that can create radicals and/or oxidants indoors has the  
118 potential to lead to secondary chemistry.<sup>27</sup> Very few studies on this topic have been conducted  
119 with state-of-the-art measurements or models. Recently, air cleaning devices based on  
120 chemistry induced by UV light (photocatalysis and OH generation, but not GUV), often also  
121 marketed as suitable for air disinfection, have been experimentally shown to produce significant  
122 amounts of OVOCs and SOA.<sup>31,32</sup>

123  
124 Despite the potential of GUV to cause secondary chemistry, to our knowledge this topic has not  
125 been studied in detail to date. Some studies of GUV inactivation effectiveness have included  
126 measurements of ozone, to assess whether any was generated.<sup>9</sup> These studies report no  
127 production of ozone when mercury vapor lamps coated to limit emission from wavelengths  
128 nearer to the ozone generating wavelength of 185 nm are used, as expected. However, some  
129 uncoated or improperly-coated lamps are commercially available, so ozone production can be a  
130 problem in some cases. In this study, we perform a first modeling evaluation of the impacts of  
131 GUV254 (assuming properly-coated lamps) and GUV222 on indoor air quality. The amounts of  
132 OVOC and SOA that can be formed in typical indoor environments are investigated.

133

134

## 135 **Materials and Methods**

136 We include the photochemistry due to GUV and subsequent radical, oxidation, and SOA  
137 formation chemistries. Given the complexity of the composition of indoor air, we simplify both  
138 the chemical species present indoors and the reaction scheme, while keeping them consistent

139 with the state-of-the-art knowledge for indoor air. Surface reactions are neglected but could be  
140 important, and should be investigated in future studies.

141  
142 The chemical mechanism for this study is a combination of the inorganic radical chemistry in an  
143 oxidation flow reactor (OFR) model<sup>20,33,34</sup> and part of the Regional Atmospheric Chemistry  
144 Mechanism (RACM)<sup>35</sup> relevant to this study. Section S1 (Supp. Info.) provides more details of  
145 the mechanism. The mechanisms are run within the open-source KinSim chemical kinetics  
146 simulator,<sup>36</sup> and are made available (See SI). We perform all simulations until a steady state is  
147 reached.

148  
149 We investigate a typical indoor space with representative indoor and urban outdoor air  
150 concentrations from the literature (Table S2). The initial concentrations of most VOCs are  
151 estimated based on McDonald et al,<sup>37</sup> with the total VOC concentration assumed to be 1.7 mg  
152 m<sup>-3</sup>, a typical value for US indoor spaces.<sup>28</sup> See Section S2 for details on species lumping and  
153 initial conditions.

154  
155 The GUV254 fixture in our simulations is based on the AeroMed LEXUS L2.1 Open.<sup>38</sup> The  
156 space irradiated by this device is 45 m<sup>3</sup>, and is placed in a room of 300 m<sup>3</sup> (volume of a typical  
157 classroom), thus the irradiated volume is 15% of the volume of the room, consistent with refs  
158 39,40. The GUV254 model has two compartments, one for the irradiated zone and the other for  
159 the rest of the room, while that for GUV222 has only one compartment. Based on the UV  
160 inactivation rate constants at 222 nm for SARS-CoV-2,<sup>6,7</sup> the UV intensity for GUV222 is  
161 adjusted such that it provides the same whole-room effective virus-removal rate as GUV254  
162 (see Section S3). Three levels of ventilation, i.e., a representative residential level (0.3 ACH,  
163 “low ventilation”),<sup>41</sup> a representative commercial level (3 ACH, “medium ventilation”),<sup>19</sup> and a  
164 representative medical level (9 ACH, “high ventilation”)<sup>3</sup> are simulated in this study. Indoor VOC  
165 emissions are set such that all VOC concentrations remain at their literature-constrained initial  
166 values at low ventilation without chemistry occurring. To test COVID-19 infection risk in different  
167 situations, we assume the presence of an infector shedding aerosolized SARS-CoV-2 at 16  
168 quanta h<sup>-1</sup> (roughly for light exercise while speaking 50% time),<sup>42</sup> which is consistent or lower  
169 than values constrained for literature superspreading events.<sup>15</sup> A quantum is an infectious dose,  
170 that if inhaled by a susceptible person, will lead to a probability of infection of 1-1/e.<sup>15,43</sup> The rate  
171 of SARS-CoV-2 loss apart from ventilation and GUV (i.e., due to intrinsic loss of infectivity,  
172 aerosol deposition etc.) is assumed to be 1 h<sup>-1</sup>.

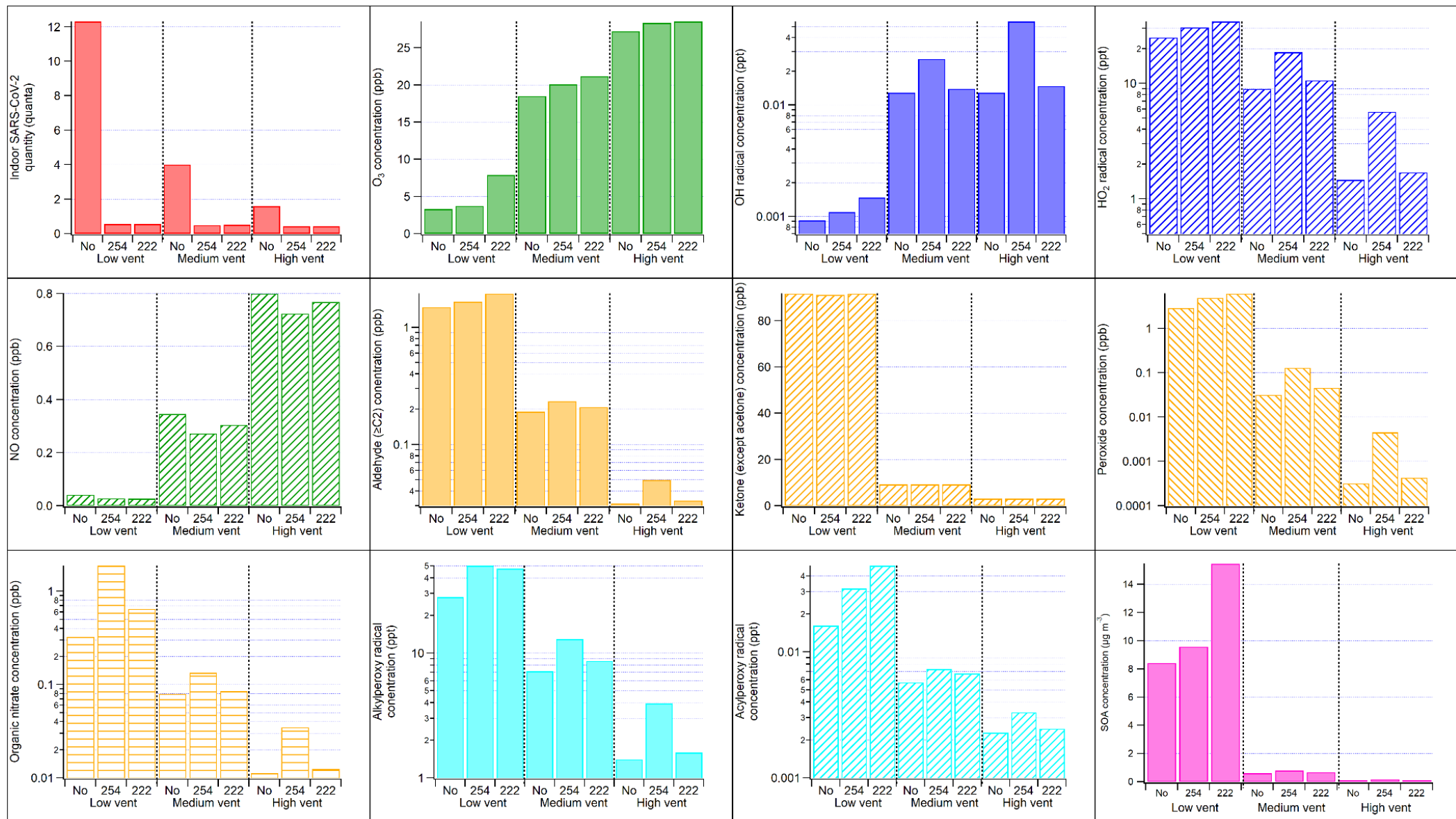
173

174

175 **Results and Discussion**

176 *Disinfection.* Figure 2 shows the amount of SARS-CoV-2 present in the room to be consistent  
177 with the steady-state prediction. In the absence of GUV, the emission rate of SARS-CoV-2 is 16  
178 quanta  $\text{h}^{-1}$ , and its total loss rate  $1.3 \text{ h}^{-1}$  ( $0.3 \text{ h}^{-1}$  from ventilation and  $1 \text{ h}^{-1}$  from decay and  
179 deposition) for the low-ventilation case. The steady state SARS-CoV-2 quantity in the entire  
180 room is 12.3 quanta. It is lowered to 4 and 1.6 quanta by increasing the ventilation rate to 3 and  
181 9 ACH, respectively. When GUV with a whole-room virus-removal rate of  $\sim 30 \text{ h}^{-1}$  is applied,  
182 SARS-CoV-2 decreases to  $\sim 0.6$ ,  $\sim 0.5$ , and  $\sim 0.4$  quanta in the low-, medium-, and high-  
183 ventilation cases, respectively. The relative impact of GUV is higher at low ventilation, as  
184 expected.

185



216  
 217 **Figure 2.** Final quantity/concentration of the main (types of) species of interest in this study under different GUV and ventilation  
 218 conditions. In the GUV254 cases, the volume-weighted average concentrations for the whole room are shown. The stable chemical  
 219 species concentrations are similar between the irradiated and unirradiated zones, while the radical and SARS-CoV-2 concentrations  
 220 in the unirradiated zone can be significantly lower and higher, respectively (Table S3). Note that some panels use log scale for  
 221 concentrations while other panels use linear scale. SOA is assumed to have a molar weight of 200 g mol<sup>-1</sup>.



222 The total quantity of SARS-CoV-2 does not directly reflect its infection risk, which also depends  
223 on the volume of the room and the inhalation by susceptible occupants. For an occupant with a  
224 breathing rate of  $0.5 \text{ m}^3 \text{ h}^{-1}$  (typical for light physical activities)<sup>44</sup> present in the  $300 \text{ m}^3$  room with  
225 low ventilation and no GUV fixture for 1 h,  $\sim 0.02$  quantum is inhaled. This corresponds to an  
226 infection probability of  $\sim 2\%$ , since the infection probability is approximately equal to the inhaled  
227 quanta if the latter is small.<sup>45</sup> For the cases studied in this work, infection risk is reduced by  $x\sim 3$   
228 by medium ventilation, and by a factor of  $\sim 22/8/4$  when adding GUV to a low/medium/high  
229 ventilation situation.

230  
231 *Secondary Chemistry.* For chemical species in the room, ventilation alone (without GUV) can  
232 make some difference (Fig. 2). The differences in  $\text{O}_3$ , NO, and ketone concentrations are largely  
233 due to these species being ventilated in or out. For other chemical species, secondary chemical  
234 processes also play a role. OH radicals can form even without UV, i.e., from limonene  
235 ozonolysis. As a result, OH radicals are higher at medium and high ventilation, which introduces  
236 more  $\text{O}_3$  from outdoors than at low ventilation. OH concentration at high ventilation is not higher  
237 than medium ventilation because high ventilation also decreases indoor limonene, reducing the  
238 overall limonene- $\text{O}_3$  reaction rate.  $\text{HO}_2$  radicals are lower at higher ventilation because of higher  
239 NO being ventilated into the room, which reacts with  $\text{HO}_2$ . All other organic radicals and stable  
240 products shown in Fig. 2 (including SOA) have higher concentrations in the low-ventilation case  
241 due to higher VOC concentrations.

242  
243 With GUV254, although the concentration of photolyzable  $\text{O}_3$  remains relatively stable (due to  
244 much stronger replenishment from outdoor air ventilation than photolytic destruction), the  
245 chemistry is significantly altered by UV (Fig. 2). The fundamental cause of this change is OH  
246 production from  $\text{O}_3$  photolysis.<sup>20</sup> OH concentrations in the GUV254 cases are approximately a  
247 factor of 1.2-5 and 3-20 times those in the corresponding no-UV cases for the whole room  
248 average and for the irradiated zone, respectively. The difference in the higher-ventilation cases  
249 is larger, due to more  $\text{O}_3$  in the room from outside air (Fig. 2 and Table S3). OH in the higher-  
250 ventilation cases is similar to daytime outdoor urban levels.<sup>46</sup> This OH level is high enough to  
251 drive substantial oxidation of VOCs, production of other radicals (e.g.,  $\text{HO}_2$  and organic peroxy  
252 radicals ( $\text{RO}_2$ )), and SOA formation. Organic peroxides (including hydroperoxides), carbonyls  
253 (aldehydes (excluding formaldehyde) and ketones (excluding acetone)), and organic nitrates  
254 (including peroxy nitrates) are among common VOC oxidation products and all have  $\sim 10\%$  to  
255 several-fold concentration increases (Fig. 2). The exceptions are ketones (excluding acetone),

256 whose production is dominated in the model by UV-independent limonene ozonolysis (Fig. 2).  
257 Doubling RH significantly increases OH concentration, but changes of product species are  
258 within 10% of the base RH results, likely due to non-linear buffering from the reaction scheme  
259 (not shown). The exceptions are ketones, which are relatively unreactive and dominated in the  
260 model by the chemistry-independent acetone emission and its dilution by ventilation (Fig. 2). In  
261 addition to VOC oxidation by OH, radicals (OH, HO<sub>2</sub>, and RO<sub>2</sub>) are also produced by active  
262 photolysis of carbonyls and peroxides at 254 nm, where both strongly absorb (Fig. 1c). Due to  
263 higher peroxy radical concentrations, NO is lowered to ~30 ppt at low ventilation (Fig. 2). Such a  
264 low NO concentration leads to reactions of RO<sub>2</sub> with both HO<sub>2</sub> and NO being important, as  
265 estimated per ref 47 (Section S4).

266  
267 SOA formation is estimated from the consumption of individual VOCs and SOA mass yields  
268 from the literature (Table S4). Significant SOA production (~8 μg m<sup>-3</sup> at low ventilation) occurs  
269 even without GUV irradiation, through limonene ozonolysis, as this reaction has a high SOA  
270 yield (20%). In the GUV254 cases, both limonene ozonolysis and VOC oxidation by OH  
271 contribute to SOA. The overall SOA mass yield from total VOC is of the order of 0.1%, because  
272 a large fraction of total organic molecules present are too small to form SOA through oxidation  
273 (e.g., ethanol or acetone). Given that 1.5 mg m<sup>-3</sup> of total VOCs (excluding limonene) are  
274 present, that leads to ~1.2 μg m<sup>-3</sup> due to GUV254. The enhancement of SOA formation by OH  
275 oxidation relative to the no-UV cases decreases with increasing ventilation, as VOC  
276 concentrations are lowered by ventilation (Fig. 2). The SOA precursors and mechanism used in  
277 this work are likely incomplete, given the incomplete scientific understanding of this topic.<sup>48</sup>

278  
279 Due to the fast air exchange between the GUV254 irradiated and unirradiated spaces, the  
280 concentrations of stable species are similar between these two spaces (Table S3). In contrast,  
281 radicals are more rapidly consumed in the unirradiated space than supplied by the transport  
282 from the irradiated space, and thus have much lower concentrations (up to >1 order of  
283 magnitude for highly reactive ones such as OH and acylperoxy) in the unirradiated space.

284  
285 The GUV222 cases assume irradiation of the entire room volume (Fig. 1b). 222 nm photons can  
286 photolyze O<sub>2</sub> and produce O<sub>3</sub>, albeit at a small rate, leading to higher O<sub>3</sub> in all cases relative to  
287 GUV254. The amounts of organic products formed in the medium- and high-ventilation (low-  
288 ventilation) cases are lower (higher) than in the unirradiated zone in the GUV254 cases (Fig. 2).

289

290 At medium and high ventilation rates, the main O<sub>3</sub> source in the GUV222 cases is still outdoor  
291 O<sub>3</sub> through ventilation. Despite some O<sub>3</sub> production, the product enhancement is much smaller  
292 than in the corresponding GUV254 cases (Fig. 2). These results indicate a weak OH-initiated  
293 VOC oxidation on top of the VOC ozonolysis chemistry that is active in the no-UV cases.

294  
295 This difference from the active photochemistry in the GUV254 cases can be attributed to several  
296 factors. First, the UV irradiance of the 222 nm fixture is significantly lower, even in terms of the  
297 number of photons emitted per unit time. 222 nm photons are ~40% more efficient in  
298 inactivating SARS-CoV-2 than 254 nm photons.<sup>6</sup> In addition the latter cannot be used in the  
299 most efficient fashion. Due to the need to protect humans from irradiation, all photons are  
300 concentrated in the small irradiated zone (15% of the room volume). Because of the limited rate  
301 of transport of virus-containing aerosol to the irradiated zone, the steady-state infectious virus  
302 concentration is ~70% lower than in the unirradiated zone, where the infector and the  
303 susceptible individuals are present (Table S3). Even if the per-photon virus-inactivation  
304 efficiency was the same, GUV254 would need about 3 times the photons for GUV222 to reach  
305 the same effective GUV virus-removal rate for the occupied unirradiated space. Furthermore,  
306 the first step of OH photochemical production is O<sub>3</sub> photolysis, whose corresponding absorption  
307 at 222 nm is about ~5 times lower than at 254 nm (Fig. 1c). Simple carbonyl compounds, the  
308 most abundant OVOCs in this study, also absorb much less efficiently at 222 nm than at 254 nm  
309 (Fig. 1c), further reducing radical production. Although other products, such as peroxides and  
310 conjugated carbonyl species, can have stronger absorption at 222 nm, their relatively low  
311 concentrations (~1 ppb or lower vs. hundreds of ppb of ketones) limit their relative contributions  
312 to the radical budget.

313  
314 Because of the small direct production of O<sub>3</sub> by the GUV222 lights, O<sub>3</sub> in the GUV222 low-  
315 ventilation case is substantially less depleted by limonene ozonolysis than for GUV254. As a  
316 result, compared to GUV254 SOA formation through limonene ozonolysis is substantially  
317 stronger and OH concentration is also higher (Fig. 2). Other gas-phase stable organic products  
318 have comparable concentrations to those in the GUV254 case.

319  
320 *Implications.* We have shown that GUV disinfection can induce active photochemistry producing  
321 OVOCs and SOA in typical indoor environments. Under the conditions simulated here, these  
322 products do not necessarily have significant negative effects on human health because of their  
323 relatively low concentrations. Among the VOCs (including OVOCs) modeled in this study, only

324 formaldehyde has a concentration exceeding the Minimal Risk Level (MRL) recommended by  
325 the CDC<sup>49</sup> due to strong indoor emissions. However, only a very limited number of species were  
326 explicitly modeled in this study, particularly aldehydes, whose toxicity is generally high. Future  
327 studies with higher chemical speciation are needed to better assess the toxicity of gas-phase  
328 products. In polluted indoor spaces and/or outdoor atmospheric environments, the indoor  
329 concentrations of the VOCs of interest can be much higher,<sup>28</sup> while the GUV-induced  
330 photochemistry can still be active (Sections S5-S6). In this case, OVOC products might exceed  
331 the MRLs and SOA formation might reach tens of  $\mu\text{g m}^{-3}$ .

332  
333 The risk of GUV254 due to secondary photochemical products is not negligible but also not  
334 dominant under typical indoor conditions. The risk for GUV222 appears to be substantially lower  
335 when ventilation is not poor, but comparable or slightly higher in case of poor ventilation. We  
336 note that many indoor environments, in particular homes and schools, have ventilation rates  
337 similar to the definition of “poor” in this paper, even in high-income countries. If GUV222 is  
338 confirmed to be safe for direct human exposure, it would have an advantage over GUV254 at  
339 mid to high ventilation rates in terms of indoor chemistry, in addition to more efficient air  
340 disinfection. When GUV254 is used, a strong air exchange between the irradiated and  
341 unirradiated zones (e.g., by fans) is preferable, as recommended by the CDC/NIOSH.<sup>50</sup> It can  
342 lower the UV irradiance needed for a given virus inactivation rate,<sup>51</sup> and hence limit the induced  
343 photochemistry. Good ventilation can not only remove airborne pathogens, but also limit the  
344 production of secondary indoor pollutants, and is thus also recommended when outdoor air is  
345 relatively clean.<sup>19,52</sup> Similarly, particulate air filtration is also recommended as it removes both  
346 virus-containing aerosol, indoor-formed SOA, and particulate pollution from other indoor and  
347 outdoor sources. Gas filtration with sorbent materials such as activated carbon is also useful for  
348 reducing VOC,  $\text{NO}_x$  and ozone levels indoors.<sup>53,54</sup> The findings of this study are limited due to  
349 modeling assumptions, e.g., the simplified chemical mechanism, limited data on photolysis  
350 parameters in the UVC range, the assumed indoor and outdoor air pollutant compositions,  
351 uncertainties over precursors and yields of SOA formation, and surface reactions. Experimental  
352 studies in both simplified laboratory settings and real indoor conditions are needed to fully  
353 constrain the impacts of GUV in indoor chemistry.

354

355

356 **Acknowledgements**

357 ZP and JLJ were supported by the CIRES Innovative Research Program and the Balvi  
358 Filantropic Fund. We thank Vito Ilacqua, Zachary Finewax, Donald Milton, and Edward Nardell  
359 for valuable discussions.

360

### 361 **Associated Content**

362 This paper has been previously submitted to medRxiv, a preprint server for health sciences. The  
363 preprint can be cited as Peng, Z.; Miller, S. L.; Jimenez, J. L. Model Evaluation of Secondary  
364 Chemistry due to Disinfection of Indoor Air with Germicidal Ultraviolet Lamps. 2022. medRxiv  
365 10.1101/2022.08.25.22279238v3 (accessed November 16, 2022).

366

### 367 **Supporting Information**

368 The Supporting Information is available free of charge at  
369 <https://pubs.acs.org/doi/10.1021/acs.estlett.xxxxxxx>.

370 Details about the model setup (reaction scheme, species lumping, indoor emission, outdoor air  
371 composition, initial conditions, effective virus-removal rates of GUV), RO<sub>2</sub> fates in the GUV254  
372 cases, concentrations in the irradiated and unirradiated zones in the GUV254 cases, and  
373 sensitivity cases for highly polluted conditions.

374

375

### 376 **References**

- 377 (1) Wells, W. F.; Wells, M. W.; Wilder, T. S. The Environmental Control of Epidemic Contagion.  
378 I. *An epidemiologic study of radiant disinfection of air in day schools* *Am J Hyg* **1942**, *35*,  
379 97–121.
- 380 (2) Riley, R. L.; Mills, C. C.; O'grady, F.; Sultan, L. U.; Wittstadt, F.; Shivpuri, D. N.  
381 Infectiousness of Air from a Tuberculosis Ward. Ultraviolet Irradiation of Infected Air:  
382 Comparative Infectiousness of Different Patients. *Am. Rev. Respir. Dis.* **1962**, *85*, 511–525.
- 383 (3) Nardell, E. A. Air Disinfection for Airborne Infection Control with a Focus on COVID-19:  
384 Why Germicidal UV Is Essential. *Photochem. Photobiol.* **2021**, *97* (3), 493–497.
- 385 (4) Riley, R. L.; Nardell, E. A. Clearing the Air: The Theory and Application of Ultraviolet Air  
386 Disinfection. *American Review of Respiratory Disease*. 1989, pp 1832–1832.  
387 <https://doi.org/10.1164/ajrccm/140.6.1832b>.
- 388 (5) Zaffina, S.; Camisa, V.; Lembo, M.; Vinci, M. R.; Tucci, M. G.; Borra, M.; Napolitano, A.;  
389 Cannatà, V. Accidental Exposure to UV Radiation Produced by Germicidal Lamp: Case  
390 Report and Risk Assessment. *Photochem. Photobiol.* **2012**, *88* (4), 1001–1004.
- 391 (6) Ma, B.; Gundy, P. M.; Gerba, C. P.; Sobsey, M. D.; Linden, K. G. UV Inactivation of SARS-  
392 CoV-2 across the UVC Spectrum: KrCl\* Excimer, Mercury-Vapor, and Light-Emitting-Diode  
393 (LED) Sources. *Appl. Environ. Microbiol.* **2021**, *87* (22), e0153221.
- 394 (7) Buonanno, M.; Welch, D.; Shuryak, I.; Brenner, D. J. Far-UVC Light (222 Nm) Efficiently  
395 and Safely Inactivates Airborne Human Coronaviruses. *Sci. Rep.* **2020**, *10* (1), 10285.
- 396 (8) Ong, Q.; Wee, W.; Cruz, J. D.; Ronnie Teo, J. W.; Han, W. 222-Nm Far UVC Exposure

- 397 Results in DNA Damage and Transcriptional Changes to Mammalian Cells. *bioRxiv*, 2022,  
398 2022.02.22.481471. <https://doi.org/10.1101/2022.02.22.481471>.
- 399 (9) Kujundzic, E.; Matalkah, F.; Howard, C. J.; Hernandez, M.; Miller, S. L. UV Air Cleaners  
400 and Upper-Room Air Ultraviolet Germicidal Irradiation for Controlling Airborne Bacteria and  
401 Fungal Spores. *J. Occup. Environ. Hyg.* **2006**, *3* (10), 536–546.
- 402 (10) Wang, C. C.; Prather, K. A.; Sznitman, J.; Jimenez, J. L.; Lakdawala, S. S.; Tufekci, Z.;  
403 Marr, L. C. Airborne Transmission of Respiratory Viruses. *Science* **2021**, *373* (6558),  
404 eabd9149.
- 405 (11) Greenhalgh, T.; Jimenez, J. L.; Prather, K. A.; Tufekci, Z.; Fisman, D.; Schooley, R. Ten  
406 Scientific Reasons in Support of Airborne Transmission of SARS-CoV-2. *Lancet* **2021**.  
407 [https://doi.org/10.1016/S0140-6736\(21\)00869-2](https://doi.org/10.1016/S0140-6736(21)00869-2).
- 408 (12) Klompas, M.; Milton, D. K.; Rhee, C.; Baker, M. A.; Leekha, S. Current Insights Into  
409 Respiratory Virus Transmission and Potential Implications for Infection Control Programs :  
410 A Narrative Review. *Ann. Intern. Med.* **2021**, *174* (12), 1710–1718.
- 411 (13) Qian, H.; Miao, T.; Liu, L.; Zheng, X.; Luo, D.; Li, Y. Indoor Transmission of SARS-CoV-  
412 2. *Indoor Air* **2020**, in press.
- 413 (14) Adam, D. C.; Wu, P.; Wong, J. Y.; Lau, E. H. Y.; Tsang, T. K.; Cauchemez, S.; Leung,  
414 G. M.; Cowling, B. J. Clustering and Superspreading Potential of SARS-CoV-2 Infections in  
415 Hong Kong. *Nat. Med.* **2020**, *26* (11), 1714–1719.
- 416 (15) Peng, Z.; Rojas, A. L. P.; Kropff, E.; Bahnfleth, W.; Buonanno, G.; Dancer, S. J.;  
417 Kurnitski, J.; Li, Y.; Loomans, M. G. L. C.; Marr, L. C.; Morawska, L.; Nazaroff, W.; Noakes,  
418 C.; Querol, X.; Sekhar, C.; Tellier, R.; Greenhalgh, T.; Bourouiba, L.; Boerstra, A.; Tang, J.  
419 W.; Miller, S. L.; Jimenez, J. L. Practical Indicators for Risk of Airborne Transmission in  
420 Shared Indoor Environments and Their Application to COVID-19 Outbreaks. *Environ. Sci.*  
421 *Technol.* **2022**, *56* (2), 1125–1137.
- 422 (16) Li, Y.; Cheng, P.; Jia, W. Poor Ventilation Worsens Short-Range Airborne Transmission  
423 of Respiratory Infection. *Indoor Air* **2022**, *32* (1), e12946.
- 424 (17) Jimenez, J. L.; Peng, Z.; Pagonis, D. Systematic Way to Understand and Classify the  
425 Shared-Room Airborne Transmission Risk of Indoor Spaces. *Indoor Air* **2022**, *32* (5),  
426 e13025.
- 427 (18) Morawska, L.; Allen, J.; Bahnfleth, W.; Bluysen, P. M.; Boerstra, A.; Buonanno, G.;  
428 Cao, J.; Dancer, S. J.; Floto, A.; Franchimon, F.; Greenhalgh, T.; Haworth, C.; Hogeling, J.;  
429 Isaxon, C.; Jimenez, J. L.; Kurnitski, J.; Li, Y.; Loomans, M.; Marks, G.; Marr, L. C.;  
430 Mazzarella, L.; Melikov, A. K.; Miller, S.; Milton, D. K.; Nazaroff, W.; Nielsen, P. V.; Noakes,  
431 C.; Peccia, J.; Prather, K.; Querol, X.; Sekhar, C.; Seppänen, O.; Tanabe, S.-I.; Tang, J.  
432 W.; Tellier, R.; Tham, K. W.; Wargocki, P.; Wierzbicka, A.; Yao, M. A Paradigm Shift to  
433 Combat Indoor Respiratory Infection. *Science* **2021**, *372* (6543), 689–691.
- 434 (19) ASHRAE. *Ventilation for Acceptable Indoor Air Quality: ANSI/ASHRAE Standard 62.1-  
435 2019*; ANSI/ASHRAE, 2019.
- 436 (20) Peng, Z.; Jimenez, J. L. Radical Chemistry in Oxidation Flow Reactors for Atmospheric  
437 Chemistry Research. *Chem. Soc. Rev.* **2020**, *49* (9), 2570–2616.
- 438 (21) Atkinson, R.; Arey, J. Atmospheric Degradation of Volatile Organic Compounds. *Chem.*  
439 *Rev.* **2003**, *103* (12), 4605–4638.
- 440 (22) Ziemann, P. J.; Atkinson, R. Kinetics, Products, and Mechanisms of Secondary Organic  
441 Aerosol Formation. *Chem. Soc. Rev.* **2012**, *41* (19), 6582–6605.
- 442 (23) Blitz, M. A.; Heard, D. E.; Pilling, M. J. Wavelength Dependent Photodissociation of  
443 CH<sub>3</sub>OOH: Quantum Yields for CH<sub>3</sub>O and OH, and Measurement of the OH+ CH<sub>3</sub>OOH  
444 Rate Coefficient. *J. Photochem. Photobiol. A Chem.* **2005**, *176* (1-3), 107–113.
- 445 (24) Vaghjiani, G. L.; Ravishankara, A. R. Photodissociation of H<sub>2</sub>O<sub>2</sub> and CH<sub>3</sub>OOH at 248  
446 Nm and 298 K: Quantum Yields for OH, O(3P) and H(2S). *J. Chem. Phys.* **1990**, *92* (2),  
447 996–1003.

- 448 (25) Link, M. F.; Farmer, D. K.; Berg, T.; Flocke, F.; Ravishankara, A. R. Measuring  
449 Photodissociation Product Quantum Yields Using Chemical Ionization Mass Spectrometry:  
450 A Case Study with Ketones. *J. Phys. Chem. A* **2021**, *125* (31), 6836–6844.
- 451 (26) Rajakumar, B.; Gierczak, T.; Flad, J. E.; Ravishankara, A. R.; Burkholder, J. B. The  
452 CH<sub>3</sub>CO Quantum Yield in the 248 Nm Photolysis of Acetone, Methyl Ethyl Ketone, and  
453 Biacetyl. *J. Photochem. Photobiol. A Chem.* **2008**, *199* (2-3), 336–344.
- 454 (27) Collins, D. B.; Farmer, D. K. Unintended Consequences of Air Cleaning Chemistry.  
455 *Environ. Sci. Technol.* **2021**. <https://doi.org/10.1021/acs.est.1c02582>.
- 456 (28) Logue, J. M.; McKone, T. E.; Sherman, M. H.; Singer, B. C. Hazard Assessment of  
457 Chemical Air Contaminants Measured in Residences. *Indoor Air* **2011**, *21* (2), 92–109.
- 458 (29) Mattila, J. M.; Arata, C.; Abeleira, A.; Zhou, Y.; Wang, C.; Katz, E. F.; Goldstein, A. H.;  
459 Abbatt, J. P. D.; DeCarlo, P. F.; Vance, M. E.; Farmer, D. K. Contrasting Chemical  
460 Complexity and the Reactive Organic Carbon Budget of Indoor and Outdoor Air.  
461 *Environmental Science & Technology*. 2022, pp 109–118.  
462 <https://doi.org/10.1021/acs.est.1c03915>.
- 463 (30) Price, D. J.; Day, D. A.; Pagonis, D.; Stark, H.; Algrim, L. B.; Handschy, A. V.; Liu, S.;  
464 Krechmer, J. E.; Miller, S. L.; Hunter, J. F.; de Gouw, J. A.; Ziemann, P. J.; Jimenez, J. L.  
465 Budgets of Organic Carbon Composition and Oxidation in Indoor Air. *Environ. Sci. Technol.*  
466 **2019**. <https://doi.org/10.1021/acs.est.9b04689>.
- 467 (31) Ye, Q.; Krechmer, J. E.; Shutter, J. D.; Barber, V. P.; Li, Y.; Helstrom, E.; Franco, L. J.;  
468 Cox, J. L.; Hrdina, A. I. H.; Goss, M. B.; Tahsini, N.; Canagaratna, M.; Keutsch, F. N.; Kroll,  
469 J. H. Real-Time Laboratory Measurements of VOC Emissions, Removal Rates, and  
470 Byproduct Formation from Consumer-Grade Oxidation-Based Air Cleaners. *Environmental*  
471 *Science & Technology Letters* **2021**. <https://doi.org/10.1021/acs.estlett.1c00773>.
- 472 (32) Joo, T.; Rivera-Rios, J. C.; Alvarado-Velez, D.; Westgate, S.; Lee Ng, N. Formation of  
473 Oxidized Gases and Secondary Organic Aerosol from a Commercial Oxidant-Generating  
474 Electronic Air Cleaner. *Environmental Science & Technology Letters* **2021**.  
475 <https://doi.org/10.1021/acs.estlett.1c00416>.
- 476 (33) Peng, Z.; Day, D. A.; Stark, H.; Li, R.; Lee-Taylor, J.; Palm, B. B.; Brune, W. H.;  
477 Jimenez, J. L. HO<sub>x</sub> Radical Chemistry in Oxidation Flow Reactors with Low-Pressure  
478 Mercury Lamps Systematically Examined by Modeling. *Atmospheric Measurement*  
479 *Techniques* **2015**, *8* (11), 4863–4890.
- 480 (34) Peng, Z.; Jimenez, J. L. Modeling of the Chemistry in Oxidation Flow Reactors with High  
481 Initial NO. *Atmos. Chem. Phys.* **2017**, *17* (19), 11991–12010.
- 482 (35) Stockwell, W. R.; Kirchner, F.; Kuhn, M.; Seefeld, S. A New Mechanism for Regional  
483 Atmospheric Chemistry Modeling. *J. Geophys. Res.* **1997**, *102* (D22), 25847–25879.
- 484 (36) Peng, Z.; Jimenez, J. L. KinSim: A Research-Grade, User-Friendly, Visual Kinetics  
485 Simulator for Chemical-Kinetics and Environmental-Chemistry Teaching. *J. Chem. Educ.*  
486 **2019**, *96* (4), 806–811.
- 487 (37) McDonald, B. C.; de Gouw, J. A.; Gilman, J. B.; Jathar, S. H.; Akherati, A.; Cappa, C. D.;  
488 Jimenez, J. L.; Lee-Taylor, J.; Hayes, P. L.; McKeen, S. A.; Cui, Y. Y.; Kim, S.-W.;  
489 Gentner, D. R.; Isaacman-VanWertz, G.; Goldstein, A. H.; Harley, R. A.; Frost, G. J.;  
490 Roberts, J. M.; Ryerson, T. B.; Trainer, M. Volatile Chemical Products Emerging as Largest  
491 Petrochemical Source of Urban Organic Emissions. *Science* **2018**, *359* (6377), 760–764.
- 492 (38) *Upper room germicidal ultraviolet fixtures*. AeroMed Technologies.  
493 <https://aeromed.com/product/upper-room-guv-fixtures/> (accessed 2022-02-21).
- 494 (39) Xu, P.; Kujundzic, E.; Peccia, J.; Schafer, M. P.; Moss, G.; Hernandez, M.; Miller, S. L.  
495 Impact of Environmental Factors on Efficacy of Upper-Room Air Ultraviolet Germicidal  
496 Irradiation for Inactivating Airborne Mycobacteria. *Environ. Sci. Technol.* **2005**, *39* (24),  
497 9656–9664.
- 498 (40) Xu, P.; Peccia, J.; Fabian, P.; Martyny, J. W.; Fennelly, K. P.; Hernandez, M.; Miller, S.

- 499 L. Efficacy of Ultraviolet Germicidal Irradiation of Upper-Room Air in Inactivating Airborne  
500 Bacterial Spores and Mycobacteria in Full-Scale Studies. *Atmos. Environ.* **2003**, 37 (3),  
501 405–419.
- 502 (41) Daisey, J. M.; Angell, W. J.; Apte, M. G. Indoor Air Quality, Ventilation and Health  
503 Symptoms in Schools: An Analysis of Existing Information. *Indoor Air* **2003**, 13 (1), 53–64.
- 504 (42) Buonanno, G.; Morawska, L.; Stabile, L. Quantitative Assessment of the Risk of Airborne  
505 Transmission of SARS-CoV-2 Infection: Prospective and Retrospective Applications.  
506 *Environ. Int.* **2020**, 145, 106112.
- 507 (43) Riley, E. C.; Murphy, G.; Riley, R. L. Airborne Spread of Measles in a Suburban  
508 Elementary School. *Am. J. Epidemiol.* **1978**, 107 (5), 421–432.
- 509 (44) EPA. Chapter 6—Inhalation Rates. In *Exposure Factors Handbook*; U.S. Environmental  
510 Protection Agency, 2011.
- 511 (45) Peng, Z.; Jimenez, J. L. Exhaled CO<sub>2</sub> as a COVID-19 Infection Risk Proxy for Different  
512 Indoor Environments and Activities. *Environmental Science & Technology Letters* **2021**, 8  
513 (5), 392–397.
- 514 (46) Ren, X.; Olson, J. R.; Crawford, J. H.; Brune, W. H.; Mao, J.; Long, R. B.; Chen, Z.;  
515 Chen, G.; Avery, M. A.; Sachse, G. W.; Barrick, J. D.; Diskin, G. S.; Huey, L. G.; Fried, A.;  
516 Cohen, R. C.; Heikes, B.; Wennberg, P. O.; Singh, H. B.; Blake, D. R.; Shetter, R. E.  
517 HO<sub>x</sub>chemistry during INTEX-A 2004: Observation, Model Calculation, and Comparison with  
518 Previous Studies. *J. Geophys. Res.* **2008**, 113 (D5). <https://doi.org/10.1029/2007jd009166>.
- 519 (47) Peng, Z.; Lee-Taylor, J.; Orlando, J. J.; Tyndall, G. S.; Jimenez, J. L. Organic Peroxy  
520 Radical Chemistry in Oxidation Flow Reactors and Environmental Chambers and Their  
521 Atmospheric Relevance. *Atmos. Chem. Phys.* **2019**, 19 (2), 813–834.
- 522 (48) Shrivastava, M.; Cappa, C. D.; Fan, J.; Goldstein, A. H.; Guenther, A. B.; Jimenez, J. L.;  
523 Kuang, C.; Laskin, A.; Martin, S. T.; Ng, N. L.; Petaja, T.; Pierce, J. R.; Rasch, P. J.; Roldin,  
524 P.; Seinfeld, J. H.; Shilling, J.; Smith, J. N.; Thornton, J. A.; Volkamer, R.; Wang, J.;  
525 Worsnop, D. R.; Zaveri, R. A.; Zelenyuk, A.; Zhang, Q. Recent Advances in Understanding  
526 Secondary Organic Aerosol: Implications for Global Climate Forcing. *Rev. Geophys.* **2017**,  
527 55 (2), 509–559.
- 528 (49) Hhs, U. S. Agency for Toxic Substances and Disease Registry Minimal Risk Levels  
529 [WWW Document]. URL <https://www.atsdr.cdc.gov/about/index.html> (accessed 12. 18.  
530 18) **2018**.
- 531 (50) Whalen, J. J. *Environmental Control for Tuberculosis; Basic Upper-Room Ultraviolet*  
532 *Germicidal Irradiation Guidelines for Healthcare Settings Guide*; (NIOSH) 2009-105; 2009.
- 533 (51) Riley, R. L.; Permutt, S. Room Air Disinfection by Ultraviolet Irradiation of Upper Air. Air  
534 Mixing and Germicidal Effectiveness. *Arch. Environ. Health* **1971**, 22 (2), 208–219.
- 535 (52) Morawska, L.; Tang, J. W.; Bahnfleth, W.; Bluysen, P. M.; Boerstra, A.; Buonanno, G.;  
536 Cao, J.; Dancer, S.; Floto, A.; Franchimon, F.; Haworth, C.; Hogeling, J.; Isaxon, C.;  
537 Jimenez, J. L.; Kurnitski, J.; Li, Y.; Loomans, M.; Marks, G.; Marr, L. C.; Mazzarella, L.;  
538 Melikov, A. K.; Miller, S.; Milton, D. K.; Nazaroff, W.; Nielsen, P. V.; Noakes, C.; Peccia, J.;  
539 Querol, X.; Sekhar, C.; Seppänen, O.; Tanabe, S.-I.; Tellier, R.; Tham, K. W.; Wargocki, P.;  
540 Wierzbicka, A.; Yao, M. How Can Airborne Transmission of COVID-19 Indoors Be  
541 Minimised? *Environ. Int.* **2020**, 142, 105832.
- 542 (53) Lee, P.; Davidson, J. Evaluation of Activated Carbon Filters for Removal of Ozone at the  
543 PPB Level. *Am. Ind. Hyg. Assoc. J.* **1999**, 60 (5), 589–600.
- 544 (54) Mochida, I.; Korai, Y.; Shirahama, M.; Kawano, S.; Hada, T.; Seo, Y.; Yoshikawa, M.;  
545 Yasutake, A. Removal of SO<sub>x</sub> and NO<sub>x</sub> over Activated Carbon Fibers. *Carbon N. Y.* **2000**,  
546 38 (2), 227–239.